



Light-absorption properties of brown carbon aerosols in the Asian outflow: Implications of a combination of filter and ground remote-sensing observations at Fukue Island, Japan

Chunmao Zhu ^{a,*}, Takuma Miyakawa ^a, Hitoshi Irie ^b, Yongjoo Choi ^a, Fumikazu Taketani ^a, Yugo Kanaya ^a

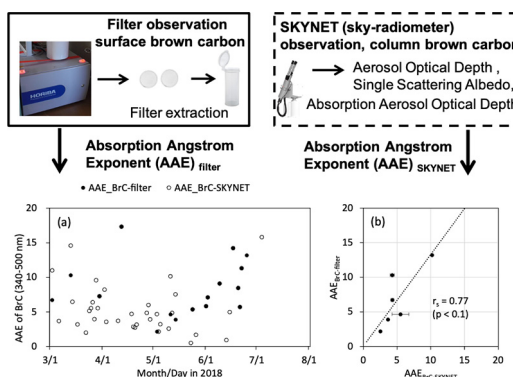
^a Research Institute for Global Change, Japan Agency for Marine-Earth Science and Technology (JAMSTEC), Yokohama 2360001, Japan

^b Center for Environmental Remote Sensing, Chiba University, Chiba 2638522, Japan

HIGHLIGHTS

- BrC light absorption was evaluated using filter and remote-sensing observations.
- The filter-based AAE was higher than the remote-sensing value by a factor of 1.33.
- A high-BrC event on Fukue was related to Asian outflow from central East China.

GRAPHICAL ABSTRACT



ARTICLE INFO

Article history:

Received 31 May 2021

Received in revised form 14 July 2021

Accepted 16 July 2021

Available online 20 July 2021

Editor: Pingqing Fu

Keywords:

Brown carbon aerosol

Light-absorption coefficient

Absorption aerosol optical depth

Absorption angstrom exponent

Sky radiometer

Filter observation

ABSTRACT

Brown carbon (BrC) aerosols have important warming effects on Earth's radiative forcing. However, information on the evolution of the light-absorption properties of BrC aerosols in the Asian outflow region is limited. In this study, we evaluated the light-absorption properties of BrC using in-situ filter measurements and sky radiometer observations of the ground-based remote sensing network SKYradiometer NETWORK (SKYNET) made on Fukue Island, western Japan in 2018. The light-absorption coefficient of BrC obtained from filter measurements had a temporal trend similar to that of the ambient concentration of black carbon (BC), indicating that BrC and BC have common combustion sources. The absorption Angstrom exponent in the wavelength range of 340–870 nm derived from the SKYNET observations was 15% higher in spring (1.81 ± 0.30) than through the whole year (1.53 ± 0.50), suggesting that the Asian outflow carries light-absorbing aerosols to Fukue Island and the western North Pacific. After eliminating the contributions of BC, the absorption Angstrom exponent of BrC alone obtained from filter observations had a positive Spearman correlation ($r_s = 0.77$, $p < 0.1$) with that derived from SKYNET observations but 33% higher values, indicating that the light-absorption properties of BrC were successfully captured using the two methods. Using the atmospheric transport model FLEXPART and fire hotspots obtained from the Visible Infrared Imaging Radiometer Suite product, we identified a high-BrC event related to an air mass originating from regions with consistent fossil fuel combustion and sporadic open biomass burning in central East China. The results of the study may help to clarify the dynamics and climatic effects of BrC aerosols in East Asia.

© 2021 Elsevier B.V. All rights reserved.

* Corresponding author.

E-mail address: chmzhu@jamstec.go.jp (C. Zhu).

1. Introduction

Light-absorbing carbonaceous aerosols are major aerosol constituents contributing to the radiative balance. It has long been realized that black carbon (BC) aerosols absorb solar radiation from ultraviolet to visible and near-infrared wavelengths, having a warming effect (Liu et al., 2020; Quinn et al., 2008). Meanwhile, organic aerosols have been deemed to cool the Earth's surface (Fuzzi et al., 2006; Zhu et al., 2019b). However, recent studies have revealed that some fraction of organic aerosols, termed brown carbon (BrC), is highly light absorbing in the ultraviolet to visible spectrum (Kirchstetter et al., 2004; Laskin et al., 2015). Global model studies have indicated that BrC accounts for ~25% to ~35% of radiative forcing by absorbing carbonaceous aerosols in the tropopause globally (Zeng et al., 2020; Zhang et al., 2020; Zhang et al., 2017). However, the role of BrC in the radiative balance remains largely uncertain, especially at the regional scale (Zhang et al., 2020). To better constrain radiative transfer models for the more accurate prediction of the future climate, it is of fundamental importance to unravel the sources, chemical composition, and optical properties of BrC.

BrC aerosols are primarily emitted in the combustion of biomass, solid fuels, and fossil fuels (Chakrabarty et al., 2010; Laskin et al., 2015). BrC chromophores can also be generated via the photo-oxidation of toluene in the presence of NO_x (Lin et al., 2015). The reaction of ammonia with secondary organic aerosols is another source of BrC (Galloway et al., 2009; Lin et al., 2015; Updyke et al., 2012). Recent studies have indicated that BrC also forms from ketoaldehydes of biogenic monoterpenes (Nguyen et al., 2013). A field study indicated that the half-life time of BrC in the atmosphere during the burning of biomass is 9–15 h (Forrister et al., 2015), although it varies for different cases.

BrC aerosols comprise of a variety of chemical components including all light-absorbing chromophores. Chemical components of BrC have been quantified through online mass spectrometry using a high-resolution time-of-flight aerosol mass spectrometer, where the H:C ratio is related to the primary sources and the O:C ratio is related to the secondary sources (Chen et al., 2016; Costabile et al., 2017). However, it is challenging to determine the chemical compound in detail. BrC chromophores can also be determined using extract-based methods, including fluorescence spectroscopy and mass spectrometry (Budisulistiorini et al., 2017; Phillips and Smith, 2015; Wu et al., 2020). The excitation-emission matrix can be derived through fluorescence spectroscopy, where BrC is often categorized as humic-like and protein-like chromophores (Chen et al., 2016; Wu et al., 2020).

In comparison with the investigation of chemical components, the investigation of the optical properties of BrC is more convenient with respect to the climatic effects. Light absorption parameters, such as the absorption coefficient (Abs), mass absorption efficiency, and absorption Angstrom exponent (AAE), are frequently quantified (Bluvshstein et al., 2017; Hecobian et al., 2010; Xie et al., 2016). Abs of BrC particles can be quantified continuously using a photoacoustic spectrometer and aethalometer (Bluvshstein et al., 2017; Saleh et al., 2013; Wang et al., 2016; Yuan et al., 2016). BrC light absorption can also be quantified by collecting aerosol samples followed by solvent extraction and measurement (Chen et al., 2016; Hecobian et al., 2010; Xie et al., 2016). Ground-based remote sensing is another option with which to evaluate BrC optical properties, although the separation of BrC from BC, mineral dust, ammonium sulfate-like components, and aerosol water is required (Bahadur et al., 2012; Choi and Ghim, 2016; Choi et al., 2020; Li et al., 2013).

Rapid economic growth in East Asian countries such as China is accompanied by large emissions of carbonaceous aerosols. A series of emission control policies has been implemented in China since 2010; e.g., the Action Plan on the Prevention and Control of Air Pollution (State Council of the People's Republic of China, 2013). As a consequence, the direct anthropogenic emission of carbonaceous aerosols in China has had a decreasing trend since 2010 (Kanaya et al., 2020;

Zheng et al., 2018). However, nonmethane volatile organic compounds increased over the period 2010–2017 (Li et al., 2019), which might foster the secondary formation of BrC. BrC can also be emitted in the burning of crop residues in China and forest fires in Russia (Zhu et al., 2015a; Zhu et al., 2017); the latter has been predicted to occur more frequently in 2100 (Veira et al., 2016). BrC from these potential sources can be transported to the outflow region in the western North Pacific, reducing the air quality, altering the aerosol chemical composition (Zhu et al., 2019a; Zhu et al., 2015b), and affecting the regional climate. However, the temporal variations and sources of BrC aerosols in the western North Pacific remain under-examined.

In this study, the light-absorption properties of BrC are investigated by combining in-situ filter measurements and sky radiometer observations made in 2018 on Fukue Island, western Japan, an outflow site of the Asian continent. We report important light-absorption properties of BrC, such as Abs obtained from filter observations, the absorption aerosol optical depth (AAOD) obtained from sky radiometer measurements, and the AAE obtained using both methods. We also report potential sources of BrC using the atmospheric Lagrangian dispersion model FLEXPART together with fire hotspots obtained from the Visible Infrared Imaging Radiometer Suite (VIIRS) satellite product.

2. Materials and methods

2.1. Observation site

Atmospheric observations were conducted at the Fukue Atmospheric Environment Observatory (32.75° N, 128.68° E, 75 m above sea level) located on Fukue Island (326.43 km²) in western Japan facing the East China Sea (Fig. 6), which is ca. 700–800 km to the east of the Asian continent (Shandong and Jiangsu provinces, China). The observatory is located on the northwestern rim of the island and is far (~23 km) from the main town on the island. Local emissions from the island thus have little effect on atmospheric observations. Under the effect of the East Asian Monsoon, the island is seasonally affected by the Asian outflow in winter and spring under westerly winds (Fig. S1), in which air pollutants were brought about (Ikeda et al., 2014; Kanaya et al., 2016; Kanaya et al., 2020; Miyakawa et al., 2019; Miyakawa et al., 2017; Takami et al., 2005).

2.2. Filter-based observations

Ambient $\text{PM}_{2.5}$ samples were collected using a continuous $\text{PM}_{2.5}$ mass and elemental concentration monitor (PX375, Horiba Ltd., Kyoto, Japan), which was deployed for the observation of particulate matter and elemental composition (Asano et al., 2017). In this study, we focus on the light-absorption properties of BrC and use the monitor only as an air sampler. A cyclone inlet (URG-2000-30EH, URG, Co., Chapel Hill, NC, USA) was installed in front of the sampler to collect $\text{PM}_{2.5}$ aerosols. Automatic sample collection was conducted at a flow rate of 16.7 L min⁻¹ for 4 h for each sample from March 1 to July 30, 2018. A rolling-type filter (polytetrafluoroethylene filter + non-woven fabric, TFH-01 L, 40 mm × 21 mm, Horiba, Ltd., Japan) was used to collect particles on a spot with a diameter of ~10 mm for each moving step. The uncollected region of the filter part was used as the field blank. Two spots collected during daytime (8:00–12:00 and 12:00–16:00 local time, LT) on a day were integrated as one sample. A total of 45 samples and three field blanks were selected for light absorption analyses. After collection, the samples were separated and stored at approximately –20 °C before analysis. Samples were handled within clean booth following relative procedures when analyzing organic molecular compounds in aerosols (Zhu et al., 2015a).

Previous studies on proper solvents for the effective extraction of BrC on filters indicated that the extraction efficiency is much higher when using methanol than when using water (Cheng et al., 2016; Xie et al., 2020; Zeng et al., 2020), although some fraction of BrC is insoluble

in methanol (Bai et al., 2020). We thus used methanol for extraction. For each sample, the filter spots were cut and extracted using 10 mL methanol (HPLC grade, Fujifilm Wako Corp., Japan) under ultrasonication for 30 min with brief intermittent manual shaking of the extraction vial. To remove BC and other relatively large particles such as dust that might interfere with the light absorption measurement of BrC, the extracts were then filtered through a syringe filter with a diameter of 13 mm and pore size of 0.2 μm (polytetrafluoroethylene for organics, Shimadzu Ltd., Japan). Although BC particles smaller than 0.2 μm could pass through the syringe filter, we found that there was no relation between the BC concentration and light absorption of extracts at wavelengths longer than 700 nm, indicating that the fraction of BC in the solvent makes a negligible contribution to the subsequently obtained light absorption.

The light absorption of the extracts was then measured using a ultraviolet–visible spectrometer (U-2910, Hitachi Ltd., Japan) over the wavelength range of 200–900 nm with a resolution of 1 nm. The obtained liquid-phase absorption (A_λ) was corrected for instrumental detection bias by subtracting the mean absorption at 795–805 nm and for the field blanks. The corresponding Abs_λ of BrC was calculated using A_λ in the ultraviolet–visible light region (300–600 nm) as

$$Abs_\lambda = A_\lambda \times \frac{V_i}{V_a \times L} \ln(10), \quad (1)$$

where V_i (m^3) is the volume (10 mL) of methanol used for extraction, V_a is the volume of sampled air ($1 \text{ m}^3 \text{ h}^{-1}$ by 8 h for two spots in a daily sample), L is the optical path length (0.01 m), and the factor $\ln(10)$ is used to convert to the natural log for consistency with the atmospheric conditions (Hecobian et al., 2010; Xie et al., 2019). A typical curve of Abs of the methanol extract in the wavelength range of 300–600 nm is shown for March 2, 2018 in Fig. 1a. The figure shows that Abs had a clear wavelength dependence with higher absorbances at shorter wavelengths. Abs at a wavelength of 365 nm (Abs_{365} , mean value of 361–370 nm) was used as a representative light-absorption coefficient for BrC.

The dependency of BrC light absorption on the wavelength based on the filter extraction method, $AAE_{BrC-filter}$, is determined as the slope of the linear fit of $\log_{10}(Abs_\lambda)$ versus $\log_{10}(\lambda)$. This study estimates $AAE_{BrC-filter}$ in the wavelength range of 340–500 nm.

2.3. Ground remote-sensing observations

Ground-based remote-sensing observations of aerosol optical properties were conducted using a sky radiometer, which was integrated

with the SKYNET observation network (Nakajima et al., 2020; Nakajima et al., 2007; Takamura, 2004). The aerosol optical depth (AOD), single-scattering albedo (SSA), Angstrom exponent (AE), volume size distribution, and refractive index were retrieved at 340, 380, 400, 500, 675, and 870 nm in 2018, using the sky radiometer analysis package of the Center for Environmental Remote Sensing (SR-CERES) version 1 (Irie et al., 2019; Mok et al., 2018). As the main program, SKYRAD.pack version 5 is implemented in SR-CERES to retrieve aerosol properties (Hashimoto et al., 2012).

To reduce uncertainty, the retrieved data were first screened to keep only those data flagged as being unaffected by cloud and having a solar zenith angle of at least 50° and then screened to keep only those data for which the SSA was less than 0.95. The AOD and SSA data were screened to keep only those larger than their uncertainties, which were assumed as 0.01 and 0.05, respectively (Irie et al., 2019). The AAOD over the whole column was then derived as

$$AAOD_\lambda = AOD_\lambda \times (1 - SSA_\lambda). \quad (2)$$

This AAOD, however, incorporates contributions from all light-absorbing particles. The corresponding AAE, denoted $AAE_{Total-SKYNET}$, was then estimated as the slope of the linear fit of $\log_{10}(AAOD_\lambda)$ versus $\log_{10}(\lambda)$ in the wavelength range of 340–870 nm.

It is known that dust contributes to light absorption, especially at short wavelengths (Khatri et al., 2010; Shin et al., 2019; Zhang and Liao, 2016). Depending on the loading of dust, uncertainties are introduced when estimating the AAOD from observations made with the sky radiometer (Koike et al., 2014). Dust events were observed occasionally in the city of Fukuoka adjacent to Fuku Island (~200 km away) by the Japan Meteorological Agency. However, after the above-mentioned data screening, only one event remained, on April 15–17, 2018, which is separately discussed in Section 3.2. For the remainder of the study period, the contributions of dust to the AAOD are assumed to be negligible. Thus, the AAOD can be assumed to be the summation of the contributions of BrC and BC:

$$AAOD_\lambda = AAOD_{\lambda-BrC} + AAOD_{\lambda-BC}. \quad (3)$$

A typical example of AAOD attribution is shown in Fig. 1b. Light absorption at wavelengths longer than 700 nm is known to be mostly contributed by BC (Kirchstetter et al., 2004). A common value of 1.0 for the AAE of BC (AAE_{BC}) has been used in fractionation studies of carbonaceous aerosols (Bond et al., 2013; Lu et al., 2015; Pani et al., 2021). In this study, assuming a value of 1.0 for AAE_{BC} and a negligible

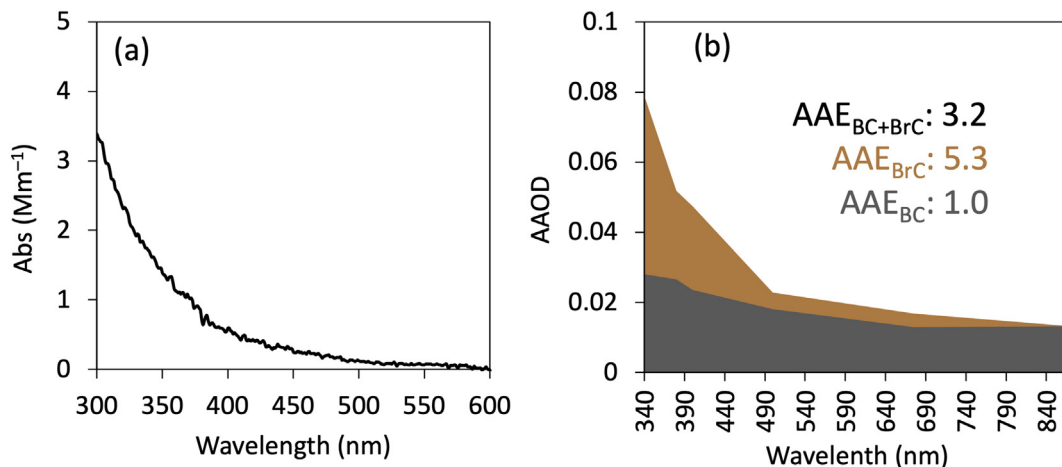


Fig. 1. Example light-absorption properties of BrC showing a dependence on wavelength, evaluated as (a) the light-absorption coefficient of methanol extracts of filter samples collected on March 2, 2018 and (b) the AAOD derived from sky radiometer observations made on January 20, 2018. The contributions of BrC were derived by assuming an AAE value of 1.0 for BC.

contribution of BrC to $AAOD_{870\text{ nm}}$, $AAOD_{\lambda-BC}$ at wavelengths shorter than 870 nm can be extrapolated as

$$AAOD_{\lambda-BC} = AAOD_{870\text{ nm}} \times \left(\frac{\lambda}{870}\right)^{-AAE_{BC}} \quad (4)$$

Summarizing Eqs. (3) and (4), $AAOD_{\lambda-BrC}$ is written as

$$AAOD_{\lambda-BrC} = AAOD_{\lambda} - AAOD_{870\text{ nm}} \times \left(\frac{\lambda}{870}\right)^{-AAE_{BC}} \quad (5)$$

The AAE contributed solely by BrC obtained by the sky radiometer ($AAE_{BrC-SKYNET}$) is then determined as the slope of the linear fit of $\log_{10}(AAOD_{\lambda-BrC})$ versus $\log_{10}(\lambda)$ in the wavelength range of 340–500 nm. To further reduce uncertainty, light-absorption properties based on sky radiometer observations were calculated as daily means for the period 9:00–15:00 LT (Irie et al., 2019).

2.4. Observation of BC

Atmospheric BC was co-investigated with BrC. The BC was observed using two filter-based instruments, namely a continuous soot monitoring system (COSMOS, model 3130, Kanomax Japan, Inc., Osaka, Japan) having a cross section of $10\text{ m}^2\text{ g}^{-1}$ at a wavelength of 565 nm and a multi-angle absorption photometer (MAAP, model 5012; Thermo Fisher Scientific, Waltham, Massachusetts, USA) having a cross section of $6.6\text{ m}^2\text{ g}^{-1}$ at a wavelength of 639 nm. The BC derived by these two instruments well agrees with values obtained using a single-particle soot photometer (SP2, Droplet Measurement Technologies, Boulder, CO, USA) and thermal optical transmittance analyzer (Sunset Laboratory, Tigard, OR, USA) (Kondo et al., 2011). Thus, the effect of BrC on the observations of BC can be ignored. We used the arithmetic mean of the BC level observed by the two instruments; this approach was validated by systematic uncertainty and random uncertainty of $\pm 14\%$ and $\pm 17\%$, respectively (Kanaya et al., 2020).

2.5. Atmospheric transport model and fire hotspots

For a high-BrC event, the footprints of air masses were evaluated using the FLEXPART Lagrangian particle dispersion model (Grythe et al., 2017; Stohl et al., 2005; Stohl et al., 1998). FLEXPART version 10.4 was run as a backward model in which the potential emission sensitivity of the receptor point, expressed as the residence time (s) in each cell, is calculated (Seibert and Frank, 2004). Meteorological data from the European Centre for Medium-Range Weather Forecasts were

operationally reanalyzed to a time resolution of 3 h at a spatial resolution of $1^\circ \times 1^\circ$ with 61 vertical levels as input. During simulation, the settings regarding dry deposition and wet scavenging were parameterized following the settings of BC, as BrC has source fractions similar to those of BC and it is difficult to fully account for the hygroscopic properties of BrC. VIIRS 375 m active fire product data were used to evaluate the intensity of the open burning of biomass during the study period (Schroeder et al., 2014). Only fire hotspot data with a high level of confidence associated with a saturated temperature anomaly were used, and those for vegetation burning sources were kept. The fire radiative power at each of the hotspots was used to indicate the fire strength.

3. Results and discussion

3.1. Filter-based BrC light absorption

The light-absorption property of BrC, Abs_{365} , co-varied with BC in March–July 2018 (Fig. 2a), with a significant Spearman correlation ($r_s = 0.61$, $p < 0.0001$) (Fig. 2b). Such a result indicates that BrC and BC have similar source regions and sectors. Abs_{365} lay in the range of $0.01\text{--}1.62\text{ Mm}^{-1}$ and had a mean \pm standard deviation of $0.58 \pm 0.43\text{ Mm}^{-1}$ (Fig. 2a). This result is in accordance with the result of a field study (mean value of 0.52 Mm^{-1}) carried out at a site similarly being far from anthropogenic pollution sources, in the southeastern United States (Xie et al., 2019). In contrast, Abs_{365} on Fukue Island in this study is one order of magnitude lower than values observed in the upper flow region at urban sites close to anthropogenic sources in Beijing (7.10 Mm^{-1} in winter 2011) and Nanjing (7.13 Mm^{-1} in spring 2018), China (Cheng et al., 2016; Xie et al., 2020). Moreover, our estimation is 1.5–2 orders of magnitude lower than measurements made close to the sources of urban emissions in Athens, Greece (annual mean, 15 Mm^{-1}) (Liakakou et al., 2020) and those made close to the sources of agricultural burning and forest fires in Thailand (Pani et al., 2021), both of which were estimated using an aethalometer. Higher BrC Abs_{365} levels are observed close to BrC emission sources, while the values reported in this work provide a reference for general BrC features in the outflow region of the Asian continent.

3.2. Aerosol light-absorption parameters obtained with the sky radiometer

Temporal variations in the AOD, SSA, and AE along with calculated AAOD and AAE retrieved from sky radiometer observations in 2018 are shown in Fig. 3. A mean AAOD of 0.09 ± 0.04 at a wavelength of 340 nm was estimated for spring, along with identifiable high-AAOD events. Meanwhile, the mean value of $AAE_{Total-SKYNET}$ in spring ($1.81 \pm$

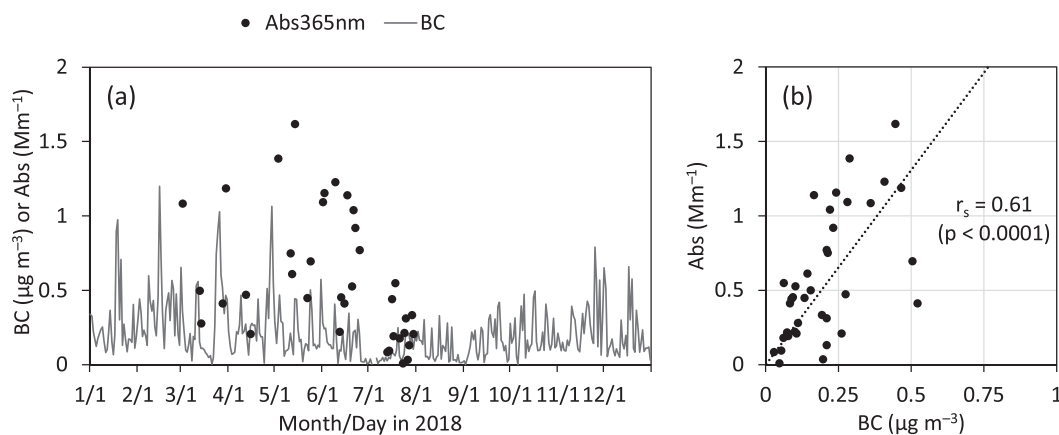


Fig. 2. Light-absorption coefficient of BrC at 365 nm (mean values for wavelengths of 360–370 nm, $Abs_{365\text{ nm}}$) and BC at Fukue in 2018: (a) temporal variations and (b) correlations. The plots show $Abs_{365\text{ nm}}$ quantified in March–July and hourly BC in the daytime (9:00–15:00 LT). The dotted line shows the linear relations, while r_s represents Spearman correlation coefficient as the data follow non-normal distribution.

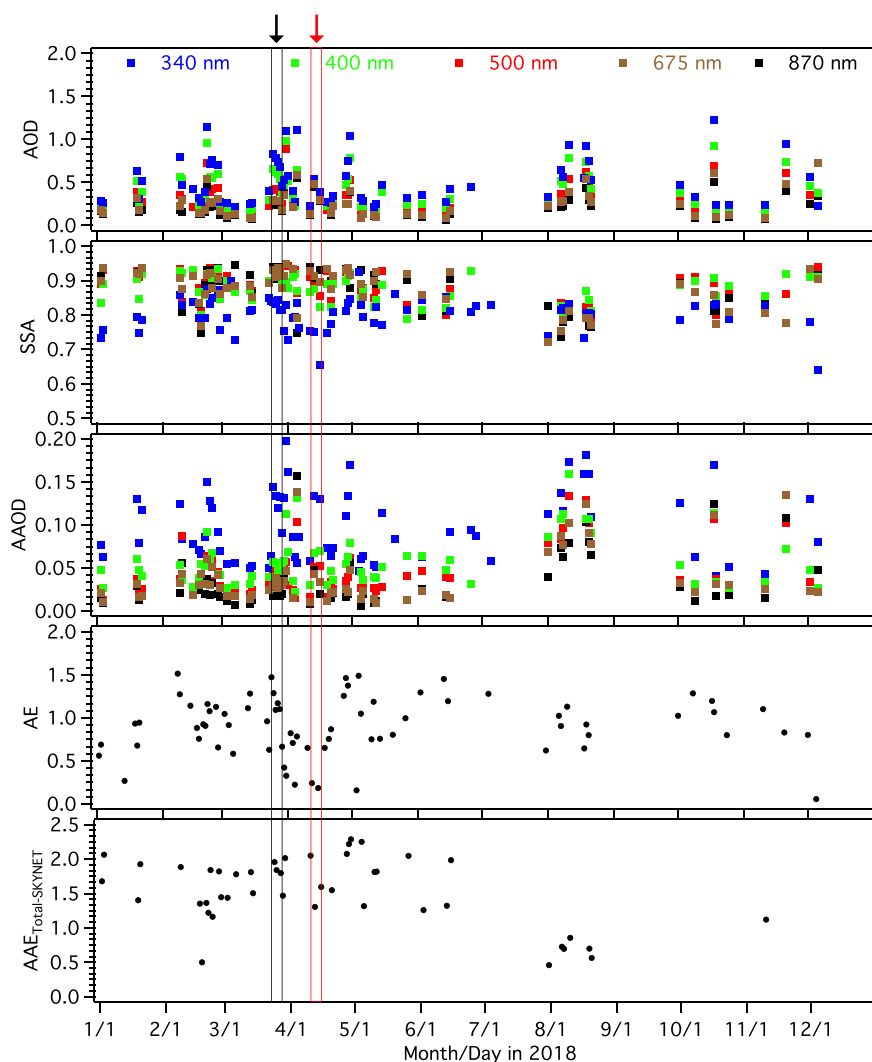


Fig. 3. Temporal variations in aerosol light absorption parameters based on SKYNET ground remote-sensing observations made in 2018. Daily means (9:00–15:00 LT) of the AOD, SSA, AAOD, AE, and $AAE_{Total-SKYNET}$ are shown. Note that $AAE_{Total-SKYNET}$ was estimated for the wavelength range of 340–870 nm and incorporates contributions from all particle types in the vertical air column, such as BrC, BC, and dust. Typical events of BrC on March 28–30 and dust on April 12–15 are indicated by black and red arrows, respectively.

0.30) was 15% higher than the mean value over the whole year (1.53 ± 0.50). It is suggested that the Asian outflow, prevailing in spring, carries light-absorbing aerosols to Fukue Island and the western North Pacific region, a phenomenon that is also observed in Gosan, Korea (Kirillova et al., 2014).

It is worth noting that the calculated AAOD and corresponding $AAE_{Total-SKYNET}$ include contributions from light-absorbing particles other than carbonaceous aerosols, such as those from dust. As an example, a transboundary dust event was observed on April 15–17, 2018 in a broad region of western Japan by the Japan Meteorological Agency. Meanwhile, a very low AE of 0.20–0.23 was estimated on April 12–15, 2018, along with a prevalent distribution of coarse mode particles (Fig. 4). Low AE values have frequently been associated with a large fraction of coarse particles (Dey et al., 2004; Gkikas et al., 2016; Gkikas et al., 2021; Tafuro et al., 2006). Although relatively high AOD and AAOD were observed at the same time, it is likely that they were due to a dust event. An AE value of 0.38 has been estimated for Gosan, Korea in April 2001 in the case of a typical dust event arriving from the Asian continent (Kim et al., 2005). When estimating the AAE of BrC (AAE_{SKYNET}) in the present study, data for days with an AE lower than 0.38 were screened out to eliminate the effect of dust.

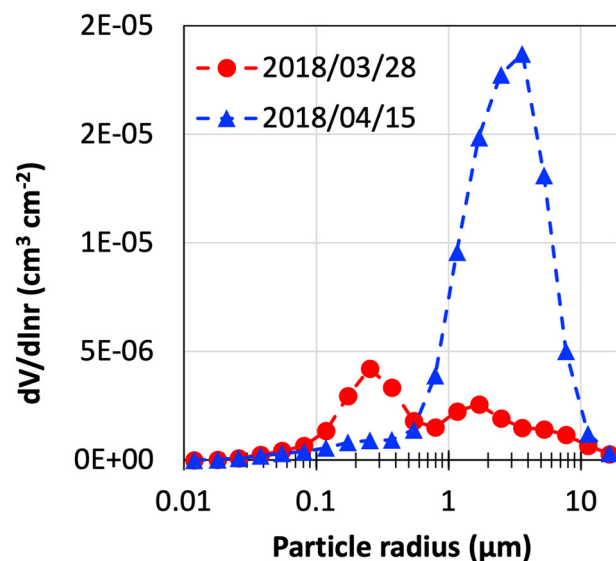


Fig. 4. Volume size distribution in an Asian dust event (April 15, 2018) and high-BrC event (March 28, 2018) as observed by a SKYNET sky radiometer.

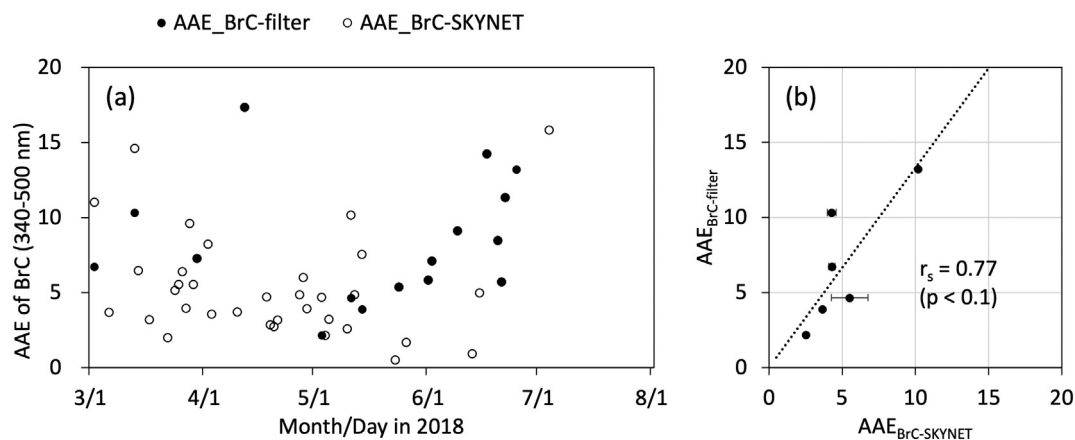


Fig. 5. $AAE_{BrC-filter}$ and $AAE_{BrC-SKYNET}$ contributed solely by BrC estimated for the wavelength range of 340–500 nm: (a) temporal variations in March–July 2018 and (b) correlations. The error bars in panel (b) are estimated by assuming that AAE_{BC} has a range of 0.8–1.4. The dotted line shows the linear relations in panel (b), while r_s represents Spearman correlation coefficient as the data follow non-normal distribution.

3.3. Comparison of the light absorptions obtained in filter and sky radiometer measurements

$AAE_{BrC-filter}$ had a variation consistent with that of $AAE_{BrC-SKYNET}$ (Fig. 5). This agreement results from the strict screening of SKYNET retrieved data, with the potential effects of dust and other uncertainties during measurement largely being eliminated. Interestingly, $AAE_{BrC-filter}$ is 33% higher than $AAE_{BrC-SKYNET}$. This difference might relate primarily to the nature of the evaluation methods. $AAE_{BrC-filter}$ reflects the wavelength dependence of particle absorption near the ground while $AAE_{BrC-SKYNET}$ incorporates that in the whole atmospheric vertical column. If particles with less light-absorbing potential at shorter wavelengths are dominant in higher layers of the column, $AAE_{BrC-SKYNET}$ lower than $AAE_{BrC-filter}$ would be estimated.

The difference between $AAE_{BrC-filter}$ and $AAE_{BrC-SKYNET}$ might also be attributed to the assumption that $AAE_{BC} = 1.0$ when estimating $AAE_{BrC-SKYNET}$. AAE_{BC} varies in the range of 0.8–1.4 depending on the source section, particle size, and mixing state (Bond et al., 2013; Lu et al., 2015; Pani et al., 2021). If the plume detected by the sky radiometer contains BC with an AAE lower than 1.0, then AAE_{SKYNET} would be underestimated. A recent study obtained a typical AAE value of 0.90, instead of 1.0, for aged BC (Liu et al., 2018). Considering a typical air-mass time of travel from the Asian continent to Fukue Island of 40 h during October to May (Kanaya et al., 2016), the real AAE of BC in the atmospheric vertical column might be lower than 1.0. In considering aerosol fractions other than BC, BrC and dust, it is noted that ammonium sulfate-like components and aerosol water having large volume fractions (Li et al., 2013) contribute to the AOD and SSA and hence $AAE_{Total-SKYNET}$, and they may introduce uncertainties in the evaluation of $AAE_{BrC-SKYNET}$.

Meanwhile, $AAE_{BrC-filter}$ was estimated on the basis of $PM_{2.5}$ sample collection whereas $AAE_{BrC-SKYNET}$ was estimated for the whole particle size range. Even though a data screen scheme was applied to sky radiometer data to reduce the effect of coarse particles by applying a threshold to the AE, it is still possible that coarse particles with low light-absorption potentials exist in the column; e.g., those mixing with BC with relatively small absorption capability (Choi et al., 2016). However, the results support the validity of sky radiometer data while suggesting that there is space for improving the correspondence to the surface value.

3.4. High-BrC event

A high-BrC event was identified with elevations of light-absorbing properties in the period March 28–30, 2018. During this event, high

levels of average Abs (0.80 Mm^{-1} , >70% percentile level for March–July, same for the following), $AAOD_{340nm}$ (0.12), $AAE_{BrC-filter}$ (7.29), and $AAE_{BrC-SKYNET}$ (7.58) were observed, along with a high BC concentration ($0.46 \mu\text{g m}^{-3}$). Meanwhile, the volume size distribution had a fine aerosol size prevalence peaking at $<1 \mu\text{m}$ for the event (Fig. 4). The air mass footprint of Fukue Island during this event originated from the North China Plain, where emissions from anthropogenic sources, such as the domestic burning of biomass and biofuels and fossil-fuel combustion, are discernable (Fig. 6). Meanwhile, fire hotspots were also observed in the region. These results suggest that besides anthropogenic emissions, open biomass burning on the North China Plain is an important source of high BrC in the outflow region. It has been reported that open burning on agricultural lands in China has reduced drastically since 2014 (Yin et al., 2021). However, the results of this study indicate that open burning in the spring of 2018 persisted as a source of BrC aerosols. This could relate to the sporadic burning of agricultural waste to clear land for spring planting, which is a main agricultural activity in the region (Liu et al., 2015; Zhang et al., 2008). As the next step, further investigations would be placed to track more evidence of BrC sources, such as using molecular organic tracers of anthropogenic sources and biomass burning.

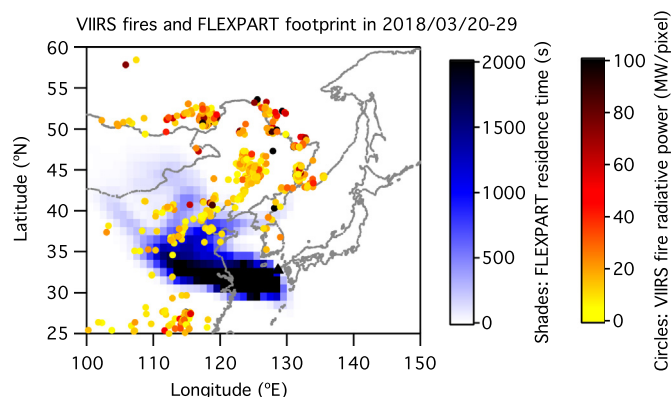


Fig. 6. Footprint of a typical high-BrC event calculated using the FLEXPART residence time during March 20–29, 2018. VIIRS fire hotspots along with fire radiative power in the same period are shown as circles. Only high-confidence VIIRS fire data for the burning of vegetation are shown. The location of the Fukue Atmospheric Environment Observatory (32.75°N , 128.68°E , 75 m above sea level) is marked as triangle. Light absorption properties of BrC based on both filter samples and ground remote-sensing observations were conducted at the same location.

4. Conclusions

We evaluated the light-absorption properties of BrC on Fukue Island through aerosol filter sampling followed by laboratory quantifications. The light-absorption coefficient of BrC co-varied with BC, indicating that BrC and BC had similar source regions and sectors. The light-absorption properties of BrC were also evaluated on the basis of sky radiometer observations following a strict data screening procedure. Correspondingly, $AAE_{BrC-filter}$ and $AAE_{BrC-SKYNET}$ of BrC had a positively linear correlation, while AAE_{filter} was 33% higher than AAE_{SKYNET} . This result shows that light-absorption properties obtained from sky radiometer observations can be converted to surface values. In the future, it is recommended to investigate the vertical distributions of aerosol light absorption properties along with size ranges. A high-BrC event on March 28–30, 2018 was identified, where air masses originated from the North China Plain with discernable open biomass burning. The results of the study clarify the dynamics and sources of BrC in East Asia.

Supplementary data to this article can be found online at <https://doi.org/10.1016/j.scitotenv.2021.149155>.

CRediT authorship contribution statement

Chunmao Zhu: Conceptualization, Methodology, Observation, Validation, Writing – Original Draft, Visualization, Funding acquisition. **Takuma Miyakawa:** Methodology, Observation, Writing – Review & Editing, Funding acquisition. **Hitoshi Irie:** Methodology, Observation, Writing – Review & Editing. **Yongjoo Choi:** Methodology, Writing – Review & Editing. **Fumikazu Taketani:** Observation, Writing – Review & Editing. **Yugo Kanaya:** Observation, Writing – Review & Editing, Supervision.

Declaration of competing interest

The authors declare that they have no known competing financial interests or personal relationships that could have appeared to influence the work reported in this paper.

Acknowledgments

The study was partly supported by Grants-in-Aid for Scientific Research (JP19K20447, JP19H04235 and JP20H04320), the Steel Foundation for Environmental Protection Technology (C-40-10 and C-48-12), the Arctic Challenge for Sustainability II (JPMXD1420318865), the Environment Research and Technology Development Fund (JPMERF20192001 and JPMERF20215005), the JAXA 2nd research announcement on the Earth Observations (19RT000351), and the Joint Research Program of CEReS, Chiba University (CJ18-17), Japan. We thank Edanz (<https://www.jp.edanz.com/ac>) for editing a draft of this manuscript.

References

- Asano, H., Aoyama, T., Mizuno, Y., Shiraishi, Y., 2017. Highly time-resolved atmospheric observations using a continuous fine particulate matter and element monitor. *ACS Earth Space Chem.* 1, 580–590.
- Bahadur, R., Praveen, P.S., Xu, Y., Ramanathan, V., 2012. Solar absorption by elemental and brown carbon determined from spectral observations. *Proc. Natl. Acad. Sci. U. S. A.* 109, 17366–17371.
- Bai, Z., Zhang, L., Cheng, Y., Zhang, W., Mao, J., Chen, H., et al., 2020. Water/methanol-insoluble brown carbon can dominate aerosol-enhanced light absorption in port cities. *Environ. Sci. Technol.* 54, 14889–14898.
- Bluvshstein, N., Lin, P., Flores, J.M., Segev, L., Mazar, Y., Tas, E., et al., 2017. Broadband optical properties of biomass-burning aerosol and identification of brown carbon chromophores. *J. Geophys. Res.-Atmos.* 122, 5441–5456.
- Bond, T.C., Doherty, S.J., Fahey, D.W., Forster, P.M., Bernsten, T., DeAngelo, B.J., et al., 2013. Bounding the role of black carbon in the climate system: a scientific assessment. *J. Geophys. Res. Atmos.* 118, 5380–5552.
- Budisulistiorini, S.H., Riva, M., Williams, M., Chen, J., Itoh, M., Surratt, J.D., et al., 2017. Light-absorbing Brown carbon aerosol constituents from combustion of Indonesian peat and biomass. *Environ. Sci. Technol.* 51, 4415–4423.

- Chakrabarty, R.K., Moosmuller, H., Chen, L.W.A., Lewis, K., Arnott, W.P., Mazzoleni, C., et al., 2010. Brown carbon in tar balls from smoldering biomass combustion. *Atmos. Chem. Phys.* 10, 6363–6370.
- Chen, Q.C., Miyazaki, Y., Kawamura, K., Matsumoto, K., Coburn, S., Volkamer, R., et al., 2016. Characterization of chromophoric water-soluble organic matter in urban, Forest, and marine aerosols by HR-ToF-AMS analysis and excitation emission matrix spectroscopy. *Environ. Sci. Technol.* 50, 10351–10360.
- Cheng, Y., He, K.-b., Du, Z.-y., Engling, G., Liu, J.-m., Ma, Y.-l., 2016. The characteristics of brown carbon aerosol during winter in Beijing. *Atmos. Environ.* 127, 355–364.
- Choi, Y., Ghim, Y.S., 2016. Estimation of columnar concentrations of absorbing and scattering fine mode aerosol components using AERONET data. *J. Geophys. Res. Atmos.* 121, 13628–13640.
- Choi, Y., Ghim, Y.S., Holben, B.N., 2016. Identification of columnar aerosol types under high aerosol optical depth conditions for a single AERONET site in Korea. *J. Geophys. Res. Atmos.* 121, 1264–1277.
- Choi, Y., Ghim, Y.S., Zhang, Y., Park, S.-M., Song, I.-h., 2020. Estimation of surface concentrations of black carbon from long-term measurements at Aeronet sites over Korea. *Remote Sens.* 12, 3904.
- Costabile, F., Gilardoni, S., Barnaba, F., Di Ianni, A., Di Liberto, L., Dionisi, D., et al., 2017. Characteristics of brown carbon in the urban Po Valley atmosphere. *Atmos. Chem. Phys.* 17, 313–326.
- Dey, S., Tripathi, S.N., Singh, R.P., Holben, B.N., 2004. Influence of dust storms on the aerosol optical properties over the indo-gangetic basin. *J. Geophys. Res. Atmos.* 109.
- Forrister, H., Liu, J., Scheuer, E., Dibb, J., Ziemba, L., Thornhill, K.L., et al., 2015. Evolution of brown carbon in wildfire plumes. *Geophys. Res. Lett.* 42, 4623–4630.
- Fuzzi, S., Andreae, M.O., Huebert, B.J., Kulmala, M., Bond, T.C., Boy, M., et al., 2006. Critical assessment of the current state of scientific knowledge, terminology, and research needs concerning the role of organic aerosols in the atmosphere, climate, and global change. *Atmos. Chem. Phys.* 6, 2017–2038.
- Galloway, M.M., Chhabra, P.S., Chan, A.W.H., Surratt, J.D., Flagan, R.C., Seinfeld, J.H., et al., 2009. Glyoxal uptake on ammonium sulphate seed aerosol: reaction products and reversibility of uptake under dark and irradiated conditions. *Atmos. Chem. Phys.* 9, 3331–3345.
- Gkikas, A., Basart, S., Hatzianastassiou, N., Marinou, E., Amiridis, V., Kazadzis, S., et al., 2016. Mediterranean intense desert dust outbreaks and their vertical structure based on remote sensing data. *Atmos. Chem. Phys.* 16, 8609–8642.
- Gkikas, A., Proestakis, E., Amiridis, V., Kazadzis, S., Di Tomaso, E., Tsekeri, A., et al., 2021. Modis dust AeroSol (MIDAS): a global fine-resolution dust optical depth data set. *Atmos. Meas. Tech.* 14, 309–334.
- Grythe, H., Kristiansen, N.I., Zwaafink, C.D.G., Eckhardt, S., Strom, J., Tunved, P., et al., 2017. A new aerosol wet removal scheme for the lagrangian particle model FLEXPART v10. *Geosci. Model Dev.* 10, 1447–1466.
- Hashimoto, M., Nakajima, T., Dubovik, O., Campanelli, M., Che, H., Khatri, P., et al., 2012. Development of a new data-processing method for SKYNET sky radiometer observations. *Atmos. Meas. Tech.* 5, 2723–2737.
- Hecobian, A., Zhang, X., Zheng, M., Frank, N., Edgerton, E.S., Weber, R.J., 2010. Water-soluble organic aerosol material and the light-absorption characteristics of aqueous extracts measured over the southeastern United States. *Atmos. Chem. Phys.* 10, 5965–5977.
- Ikeda, K., Yamaji, K., Kanaya, Y., Taketani, F., Pan, X.L., Komazaki, Y., et al., 2014. Sensitivity analysis of source regions to PM_{2.5} concentration at Fukue Island, Japan. *J. Air Waste Manag. Assoc.* 64, 445–452.
- Irie, H., Hoque, H.M.S., Damiani, A., Okamoto, H., Fatmi, A.M., Khatri, P., et al., 2019. Simultaneous observations by sky radiometer and MAX-DOAS for characterization of biomass burning plumes in Central Thailand in January–April 2016. *Atmos. Meas. Tech.* 12, 599–606.
- Kanaya, Y., Pan, X.L., Miyakawa, T., Komazaki, Y., Taketani, F., Uno, I., et al., 2016. Long-term observations of black carbon mass concentrations at Fukue Island, western Japan, during 2009–2015: constraining wet removal rates and emission strengths from East Asia. *Atmos. Chem. Phys.* 16, 10689–10705.
- Kanaya, Y., Yamaji, K., Miyakawa, T., Taketani, F., Zhu, C., Choi, Y., et al., 2020. Rapid reduction in black carbon emissions from China: evidence from 2009–2019 observations on Fukue Island, Japan. *Atmos. Chem. Phys.* 20, 6339–6356.
- Khatri, P., Takamura, T., Shimizu, A., Sugimoto, N., 2010. Spectral dependency of aerosol light-absorption over the East China Sea Region. *Sola* 6, 1–4.
- Kim, S.-W., Yoon, S.-C., Jefferson, A., Ogren, J.A., Dutton, E.G., Won, J.-G., et al., 2005. Aerosol optical, chemical and physical properties at gosan, Korea during asian dust and pollution episodes in 2001. *Atmos. Environ.* 39, 39–50.
- Kirchstetter, T.W., Novakov, T., Hobbs, P.V., 2004. Evidence that the spectral dependence of light absorption by aerosols is affected by organic carbon. *J. Geophys. Res. Atmos.* 109.
- Kirilova, E.N., Andersson, A., Han, J., Lee, M., Gustafsson, Ö., 2014. Sources and light absorption of water-soluble organic carbon aerosols in the outflow from northern China. *Atmos. Chem. Phys.* 14, 1413–1422.
- Koike, M., Moteki, N., Khatri, P., Takamura, T., Takegawa, N., Kondo, Y., et al., 2014. Case study of absorption aerosol optical depth closure of black carbon over the East China Sea. *J. Geophys. Res. Atmos.* 119, 122–136.
- Kondo, Y., Sahu, L., Moteki, N., Khan, F., Takegawa, N., Liu, X., et al., 2011. Consistency and traceability of black carbon measurements made by laser-induced incandescence, thermal-optical transmittance, and filter-based photo-absorption techniques. *Aerosol Sci. Technol.* 45, 295–312.
- Laskin, A., Laskin, J., Nizkorodov, S.A., 2015. Chemistry of atmospheric brown carbon. *Chem. Rev.* 115, 4335–4382.
- Li, Z., Gu, X., Wang, L., Li, D., Xie, Y., Li, K., et al., 2013. Aerosol physical and chemical properties retrieved from ground-based remote sensing measurements during heavy haze days in Beijing winter. *Atmos. Chem. Phys.* 13, 10171–10183.

- Li, M., Zhang, Q., Zheng, B., Tong, D., Lei, Y., Liu, F., et al., 2019. Persistent growth of anthropogenic non-methane volatile organic compound (NMVOC) emissions in China during 1990–2017: drivers, speciation and ozone formation potential. *Atmos. Chem. Phys.* 19, 8897–8913.
- Liakakou, E., Kaskaoutis, D.G., Grivas, G., Stavroulas, I., Tsagkaraki, M., Paraskevopoulou, D., et al., 2020. Long-term brown carbon spectral characteristics in a Mediterranean city (Athens). *Sci. Total Environ.* 708, 135019.
- Lin, P., Liu, J.M., Shilling, J.E., Kathmann, S.M., Laskin, J., Laskin, A., 2015. Molecular characterization of brown carbon (BrC) chromophores in secondary organic aerosol generated from photo-oxidation of toluene. *Phys. Chem. Chem. Phys.* 17, 23312–23325.
- Liu, M.X., Song, Y., Yao, H., Kang, Y.N., Li, M.M., Huang, X., et al., 2015. Estimating emissions from agricultural fires in the North China plain based on MODIS fire radiative power. *Atmos. Environ.* 112, 326–334.
- Liu, C., Chung, C.E., Yin, Y., Schnaiter, M., 2018. The absorption Ångström exponent of black carbon: from numerical aspects. *Atmos. Chem. Phys.* 18, 6259–6273.
- Liu, D.T., He, C.L., Schwarz, J.P., Wang, X., 2020. Lifecycle of light-absorbing carbonaceous aerosols in the atmosphere. *npj climate and atmospheric science* 3.
- Lu, Z., Streets, D.G., Winijkul, E., Yan, F., Chen, Y., Bond, T.C., et al., 2015. Light absorption properties and radiative effects of primary organic aerosol emissions. *Environ. Sci. Technol.* 49, 4868–4877.
- Miyakawa, T., Oshima, N., Taketani, F., Komazaki, Y., Yoshino, A., Takami, A., et al., 2017. Alteration of the size distributions and mixing states of black carbon through transport in the boundary layer in East Asia. *Atmos. Chem. Phys.* 17, 5851–5864.
- Miyakawa, T., Komazaki, Y., Zhu, C., Taketani, F., Pan, X., Wang, Z., et al., 2019. Characterization of carbonaceous aerosols in Asian outflow in the spring of 2015: importance of non-fossil fuel sources. *Atmos. Environ.* 214.
- Mok, J., Krotkov, N.A., Torres, O., Jethwa, H., Li, Z., Kim, J., et al., 2018. Comparisons of spectral aerosol single scattering albedo in Seoul, South Korea. *Atmos. Meas. Tech.* 11, 2295–2311.
- Nakajima, T., Yoon, S.C., Ramanathan, V., Shi, G.Y., Takemura, T., Higurashi, A., et al., 2007. Overview of the atmospheric Brown cloud east asian regional experiment 2005 and a study of the aerosol direct radiative forcing in East Asia. *J. Geophys. Res.-Atmos.* 112.
- Nakajima, T., Campanelli, M., Che, H., Estellés, V., Irie, H., Kim, S.W., et al., 2020. An overview of and issues with sky radiometer technology and SKYNET. *Atmos. Meas. Tech.* 13, 4195–4218.
- Nguyen, T.B., Laskin, A., Laskin, J., Nizkorodov, S.A., 2013. Brown carbon formation from ketoaldehydes of biogenic monoterpenes. *Faraday Discuss.* 165, 473–494.
- Pani, S.K., Lin, N.H., Griffith, S.M., Chantara, S., Lee, C.T., Thepnuan, D., et al., 2021. Brown carbon light absorption over an urban environment in northern peninsular Southeast Asia. *Environ. Pollut.* 276, 116735.
- Phillips, S.M., Smith, G.D., 2015. Further evidence for charge transfer complexes in brown carbon aerosols from excitation-emission matrix fluorescence spectroscopy. *J. Phys. Chem. A* 119, 4545–4551.
- Quinn, P.K., Bates, T.S., Baum, E., Doubleday, N., Fiore, A.M., Flanner, M., et al., 2008. Short-lived pollutants in the Arctic: their climate impact and possible mitigation strategies. *Atmos. Chem. Phys.* 8, 1723–1735.
- Saleh, R., Hennigan, C.J., McMeeking, G.R., Chuang, W.K., Robinson, E.S., Coe, H., et al., 2013. Absorptivity of brown carbon in fresh and photo-chemically aged biomass-burning emissions. *Atmos. Chem. Phys.* 13, 7683–7693.
- Schroeder, W., Oliva, P., Giglio, L., Csiszar, I.A., 2014. The new VIIRS 375m active fire detection data product: algorithm description and initial assessment. *Remote Sens. Environ.* 143, 85–96.
- Seibert, P., Frank, A., 2004. Source-receptor matrix calculation with a lagrangian particle dispersion model in backward mode. *Atmos. Chem. Phys.* 4, 51–63.
- Shin, S.-K., Tesche, M., Müller, D., Noh, Y., 2019. Absorption aerosol optical depth components from AERONET observations of mixed dust plumes. *Atmos. Meas. Tech.* 12, 607–618.
- State Council of the People's Republic of China, 2013. Air Pollution Prevention and Control Action Plan. (in Chinese). http://www.gov.cn/zwqk/2013-09/12/content_2486773.htm. (Accessed 21 July 2021).
- Stohl, A., Hittenberger, M., Wotawa, G., 1998. Validation of the lagrangian particle dispersion model FLEXPART against large-scale tracer experiment data. *Atmos. Environ.* 32, 4245–4264.
- Stohl, A., Forster, C., Frank, A., Seibert, P., Wotawa, G., 2005. Technical note: the lagrangian particle dispersion model FLEXPART version 6.2. *Atmos. Chem. Phys.* 5, 2461–2474.
- Tafuro, A.M., Barnaba, F., De Tomasi, F., Perrone, M.R., Gobbi, G.P., 2006. Saharan dust particle properties over the Central Mediterranean. *Atmos. Res.* 81, 67–93.
- Takami, A., Miyoshi, T., Shimono, A., Hatakeyama, S., 2005. Chemical composition of fine aerosol measured by AMS at Fukue Island, Japan during APEX period. *Atmos. Environ.* 39, 4913–4924.
- Takamura, T., 2004. Overview of SKYNET and its activities. *Opt. Pura Apl.* 37, 3303–3308.
- Updyke, K.M., Nguyen, T.B., Nizkorodov, S.A., 2012. Formation of brown carbon via reactions of ammonia with secondary organic aerosols from biogenic and anthropogenic precursors. *Atmos. Environ.* 63, 22–31.
- Veira, A., Lasslop, G., Kloster, S., 2016. Wildfires in a warmer climate: emission fluxes, emission heights, and black carbon concentrations in 2090–2099. *J. Geophys. Res.-Atmos.* 121, 3195–3223.
- Wang, X., Heald, C.L., Sedlacek, A.J., de Sa, S.S., Martin, S.T., Alexander, M.L., et al., 2016. Deriving brown carbon from multiwavelength absorption measurements: method and application to AERONET and aethalometer observations. *Atmos. Chem. Phys.* 16, 12733–12752.
- Wu, G.M., Wan, X., Ram, K., Li, P.L., Liu, B., Yin, Y.G., et al., 2020. Light absorption, fluorescence properties and sources of brown carbon aerosols in the Southeast Tibetan Plateau. *Environ. Pollut.* 257.
- Xie, M.J., Mladenov, N., Williams, M.W., Neff, J.C., Wasswa, J., Hannigan, M.P., 2016. Water soluble organic aerosols in the Colorado Rocky Mountains, USA: composition, sources and optical properties. *Sci. Rep.* 6.
- Xie, M.J., Chen, X., Holder, A.L., Hays, M.D., Lewandowski, M., Offenber, J.H., et al., 2019. Light absorption of organic carbon and its sources at a southeastern US location in summer. *Environ. Pollut.* 244, 38–46.
- Xie, X.C., Chen, Y.F., Nie, D.Y., Liu, Y., Liu, Y., Lei, R.Y., et al., 2020. Light-absorbing and fluorescent properties of atmospheric brown carbon: a case study in Nanjing, China. *Chemosphere* 251.
- Yin, S., Guo, M., Wang, X.F., Yamamoto, H., Ou, W., 2021. Spatiotemporal variation and distribution characteristics of crop residue burning in China from 2001 to 2018. *Environ. Pollut.* 268.
- Yuan, J.F., Huang, X.F., Cao, L.M., Cui, J., Zhu, Q., Huang, C.N., et al., 2016. Light absorption of brown carbon aerosol in the PRD region of China. *Atmos. Chem. Phys.* 16, 1433–1443.
- Zeng, L.H., Zhang, A.X., Wang, Y.H., Wagner, N.L., Katich, J.M., Schwarz, J.P., et al., 2020. Global measurements of Brown carbon and estimated direct radiative effects. *Geophys. Res. Lett.* 47.
- Zhang, T.-H., Liao, H., 2016. Aerosol absorption optical depth of fine-mode mineral dust in eastern China. *Atmos. Ocean. Sci. Lett.* 9, 7–14.
- Zhang, Q.Z., Yang, Z.L., Wu, W.L., 2008. Role of crop residue management in sustainable agricultural development in the North China plain. *J. Sustain. Agric.* 32, 137–148.
- Zhang, Y.Z., Forrister, H., Liu, J.M., Dibb, J., Anderson, B., Schwarz, J.P., et al., 2017. Top-of-atmosphere radiative forcing affected by brown carbon in the upper troposphere. *Nat. Geosci.* 10, 486–.
- Zhang, A.X., Wang, Y.H., Zhang, Y.Z., Weber, R.J., Song, Y.J., Ke, Z.M., et al., 2020. Modeling the global radiative effect of brown carbon: a potentially larger heating source in the tropical free troposphere than black carbon. *Atmos. Chem. Phys.* 20, 1901–1920.
- Zheng, B., Tong, D., Li, M., Liu, F., Hong, C.P., Geng, G.N., et al., 2018. Trends in China's anthropogenic emissions since 2010 as the consequence of clean air actions. *Atmos. Chem. Phys.* 18, 14095–14111.
- Zhu, C., Kawamura, K., Kunwar, B., 2015a. Effect of biomass burning over the western North Pacific rim: wintertime maxima of anhydrosugars in ambient aerosols from Okinawa. *Atmos. Chem. Phys.* 15, 1959–1973.
- Zhu, C.M., Yoshikawa-Inoue, H., Tohjima, Y., Irino, T., 2015b. Temporal variations in black carbon recorded on Rishiri Island, northern Japan. *Geochem. J.* 49, 283–294.
- Zhu, C.M., Kobayashi, H., Kanaya, Y., Saito, M., 2017. Size-dependent validation of MODIS MCD64A1 burned area over six vegetation types in boreal Eurasia: large underestimation in croplands. *Sci. Rep.* 7.
- Zhu, C., Kanaya, Y., Yoshikawa-Inoue, H., Irino, T., Seki, O., Tohjima, Y., 2019a. Sources of atmospheric black carbon and related carbonaceous components at Rishiri Island, Japan: the roles of siberian wildfires and of crop residue burning in China. *Environ. Pollut.* 247, 55–63.
- Zhu, J.L., Penner, J.E., Yu, F.Q., Sillman, S., Andreae, M.O., Coe, H., 2019. Decrease in radiative forcing by organic aerosol nucleation, climate, and land use change. *Nat. Commun.* 10.